

# Phonon Line Widths and Electron-Phonon Coupling in Nanotubes

Michele Lazzeri<sup>1</sup>, S. Piscanec<sup>2</sup>, Francesco Muzzi<sup>1</sup>, A.C. Ferrari<sup>2</sup>, and J. Robertson<sup>2</sup>

<sup>1</sup> Institut de Mécanique et de Physique des Milieux Condensés, 4 Place Jussieu, 75252, Paris cedex 05, France

<sup>2</sup> Department of Engineering, University of Cambridge, Cambridge CB2 1PZ, UK

(Dated: February 20, 2019)

We prove that Electron-phonon coupling (EPC) is the major source of broadening for the Ram an G and G<sub>0</sub> peaks in graphite and metallic nanotubes. This allows us to directly measure the optical-phonon EPCs from the G and G<sub>0</sub> line widths. The experimental EPCs compare extremely well with those from density functional theory. We show that the EPC explains the difference in the Ram an spectra of metallic and semiconducting nanotubes and their dependence on tube diameter. We discuss the common assignment of the G<sub>0</sub> peak in metallic nanotubes to a Fano resonance between phonons and plasmons. We assign the G<sup>+</sup> and G<sub>0</sub> peaks to TO (tangential) and LO (axial) modes.

PACS numbers: 73.63.Fg, 63.20.Kr, 73.22.-f

Electron-phonon coupling (EPC) is a key physical parameter in nanotubes. Ballistic transport, superconductivity, excited state dynamics, Ram an spectra and phonon dispersions all fundamentally depend on it. In particular, the optical phonons EPC are extremely relevant since electron scattering by optical phonons sets the ultimate limit to high field ballistic transport [1, 2, 3, 4, 5]. Furthermore, they play a key role in defining the phonon dispersions [6] and the Ram an spectra of metallic and semiconducting single wall nanotubes (SWNT), which show different features [7, 8, 9, 10, 11, 12, 13, 14, 15, 16, 17, 18]. Several theoretical and experimental investigations of acoustic phonons EPC have been published (see, e.g., Ref. [19]). However, only tight-binding calculations of optical phonons EPC were performed, with contrasting results [1, 2, 20, 21, 22, 23]. More crucially, no direct measurement of optical phonons EPC has been reported to validate these calculations.

In this Letter we prove that the optical phonons EPC are the major source of broadening for the Ram an G and G<sub>0</sub> peaks in graphite and metallic SWNTs. We show that the experimental Ram an line widths provide a direct EPC measurement. The EPC are also responsible for the the G<sup>+</sup> and G<sub>0</sub> splitting in metallic SWNTs. This allows us to unambiguously assign the G<sup>+</sup> and G<sub>0</sub> peaks to TO (tangential) and LO (axial) modes, in contrast to what often done [7, 8, 10, 11, 12, 15]. We discuss the common assignment of the G<sub>0</sub> peak in metallic SWNTs to a Fano resonance between phonons and plasmons [10, 11, 12, 13, 24, 25].

In a perfect crystal, the line width of a phonon is determined by its interaction with other elementary excitations. Usually,  $\omega = \omega_0 + \omega_{\text{EPC}}$ , where  $\omega_0$  is due to the interaction with other phonons and  $\omega_{\text{EPC}}$  with electron-hole pairs.  $\omega_0$  is determined by anharmonic terms in the interatomic potential and is always there.  $\omega_{\text{EPC}}$  is determined by the EPC and is present only in systems where the electron gap is zero. If the anharmonic contribution  $\omega_0$  is negligible or otherwise known, measuring the line width is the simplest way to determine the EPC.

A phonon is described by a wave vector  $q$ , branch index and frequency  $\omega_q$ . We consider a mean-field single-particle formalism, such as density functional theory (DFT) or Hartree-Fock. The EPC contribution to  $\omega_q$  is given by the Fermi golden rule [26]:

$$\frac{\omega_q}{N_k} = \frac{4}{N_k} \sum_{k,i,j} \text{Im} [f_{k,i} f_{(k+q),j}] \delta_{k,i,j} \quad (1)$$

where the sum is on the electron vectors  $k$  and bands  $i$  and  $j$ ,  $N_k$  is the number of  $k$  vectors,  $f_{k,i}$  is the occupation of the electron state  $k,i$  with energy  $\epsilon_{k,i}$ ,  $\delta_{k,i,j}$  is the Dirac distribution.  $\text{Im} [f_{k,i} f_{(k+q),j}] = D_{(k+q),j,k,i} \sim (2M \omega_q)^{-1}$ ; where  $M$  is the atomic mass.  $D_{(k+q),j,k,i} = \hbar k + q; j \text{ and } V_q \text{ is the potential derivative with respect to the phonon displacement. } D \text{ is the EPC.}$

The electron states contributing to the sum in Eq. 1 are selected by the energy conservation condition  $\epsilon_{k,i} + \omega_q = \epsilon_{(k+q),j}$ . Also, the state  $k,i$  has to be occupied and  $(k+q),j$  empty, so that the term  $[f_{k,i} f_{(k+q),j}] \neq 0$ . Thus, only electrons in the vicinity of the Fermi level contribute to  $\omega_q$ . In insulating and semiconducting systems  $\omega_q = 0$ . In general, a precise estimate of  $\omega_q$  from Eq. 1 is possible only after an accurate determination of the Fermi surface. However, graphite and SWNTs are very fortunate cases. Thanks to their particular band structure,  $\omega_q$  is given by a simple analytic formula.

In general, the EPC determines both phonon dispersions and line widths. We first consider the case of graphite and show that both dispersion and line widths give a direct measure of the EPC at  $\omega_q = 0$ .

The electron bands of graphite are well described by those of a two-dimensional graphene sheet. In graphene, the gap is zero for the bands at the two equivalent K and K' points of the Brillouin zone. We define  $\hbar D^2 = \sum_{i,j} \delta_{k,i,k,j}^2 = 4$ , where the sum is on the two degenerate bands at the Fermi level  $\omega_F$ . We consider the EPC relative to the  $E_{2g}$  phonon at  $\omega_q = 0$ . The  $E_{2g}$  mode is doubly degenerate and consists of an antiphase

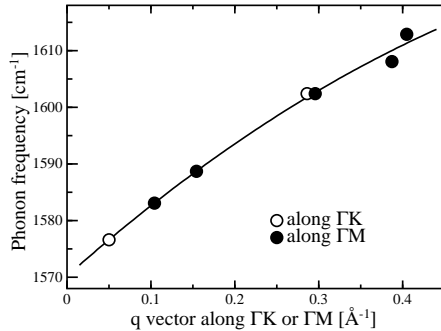


FIG. 1: Graphite phonon dispersion of the highest optical branch near  $\Gamma$ . Dots are inelastic X-ray measurements from Ref. [27]. The line is a quadratic fit.

in-plane motion. For a small non zero  $q$  near  $\Gamma$ , this splits into a quasi longitudinal (LO) and quasi transverse (TO) branch, corresponding to an atom motion parallel and perpendicular to  $q$ . From DFT calculations we get  $\hbar D^2 i_F = 45.60 \text{ (eV/Å)}^2$  for both LO and TO modes [6].

We have previously shown that graphite has two Kohn anomalies in the phonon dispersions for the  $E_{2g}$  and  $K-A_1^0$  modes [6]. Due to the anomaly, the dispersion near of the  $E_{2g}$ -LO mode is almost linear, with slope  $S^{LO}$  [6]:

$$S^{LO} = \frac{P}{8M!} \frac{3 \sim a_0^2}{\hbar D^2 i_F}; \quad (2)$$

where  $a_0 = 2.46 \text{ Å}$  is the graphite lattice spacing,  $P = 5.52 \text{ Å eV}$  is the slope of the electron bands near  $\Gamma$ ,  $M$  is the carbon atom mass and  $!$  is the frequency of the  $E_{2g}$  phonon ( $! = 196.0 \text{ meV}$ ). Eq. 2 shows that  $\hbar D^2 i_F$  can be directly measured from the experimental  $S^{LO}$ . The phonons around  $\Gamma$  have been measured by several groups with close agreement. From a quadratic fit to the most recent data of ref. [27] (Fig. 1) we get  $S^{LO} = 133 \text{ cm}^{-1} \text{ Å}$ . From Eq. 2 we have  $\hbar D^2 i_F = 39 \text{ (eV/Å)}^2$ , in good agreement with DFT.

We now show that the Full Width at Half Maximum (FWHM) of the graphite G peak gives another independent EPC measurement. The G peak of graphite is due to the  $E_{2g}$  phonon [28]. We use Eq. 1 to compute the width,  $E^P$ , for this mode. Close to  $\Gamma$ , we assume the bands dispersion to be conic from the Fermi level  $\epsilon_F$ , with slope (Fig. 2a) [29]. For both LO and TO modes:

$$E^P = \frac{P}{4M^2} \frac{3a_0^2 \sim^2}{\hbar D^2 i_F}; \quad (3)$$

We then measure FWHM (G) for a single-crystal graphite similar to that of Ref. [27]. Its Raman spectrum does not show any D peak [15, 30], thus we exclude extra broadening due to disorder [31]. By fitting the G peak with a Lorentzian we get FWHM (G) = 13 cm⁻¹. Temperature

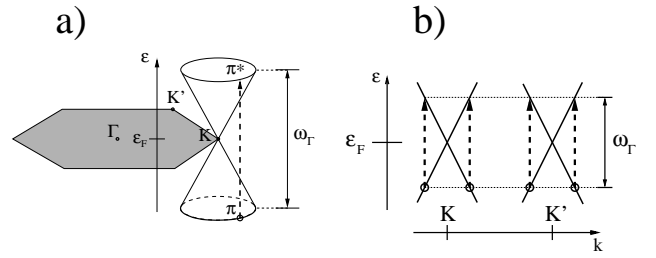


FIG. 2: Electron bands around  $K$  in graphene (a) and in a metallic tube (b). Shaded area is the graphene Brillouin zone. Dashed arrows: decay processes for a phonon.

dependent measurements show no increase of FWHM (G) in the 2K–900K range [30]. Our Raman spectrometer resolution is 1.5 cm⁻¹ [30]. We thus assume an anharmonic contribution lower than the spectral resolution  $\text{an}_G < 1.5 \text{ cm}^{-1}$ . Thus, we estimate  $E^P = 11.5 \text{ cm}^{-1}$ . Then, from Eq. 3,  $bD^2 i_F = 47 \text{ (eV/Å)}^2$ . This compares very well with DFT, again confirming that  $\text{an}_G$  is small.

Finally, near the conservation of the energy and momentum in Eq. 1, implies:

$$\frac{E^P}{q} = 0, \quad q \sim ! = : \quad (4)$$

This condition is satisfied by the  $E_{2g}$  phonon, involved in the Raman G peak of graphite. On the other hand, the double resonant mode close to  $\Gamma$ , which gives the D' peak at 1615 cm⁻¹, does not satisfy it. D' is indeed sharper than the G peak [32].

In summary, we presented two independent measurements of the graphite  $E_{2g}$  EPC. These are consistent with each other and with DFT. We now consider SWNTs.

The G peak of SWNTs can be fitted with only two components,  $G^+$  and  $G^-$  [11]. Semiconducting SWNTs have sharp  $G^+$  and  $G^-$ , whilst metallic SWNTs have a broad downshifted G [7, 8, 9, 10, 11, 12, 13, 14, 15, 16, 17, 18]. The G band shows a strong diameter dependence, being lower in frequency for smaller diameters [11]. This suggested its attribution to a tangential mode, whose circumferential atoms displacements would be most affected by a variation in diameter [10]. Thus, the  $G^+$  and  $G^-$  peaks are often assigned to LO (axial) and TO (tangential) modes [7, 8, 10, 11, 12, 15].

Contlicting reports exist on the presence and relative intensity of the G band in isolated versus bundled metallic tubes. It has been claimed that this peak is as intense in isolated SWNTs as in bundles [11, 17, 18]; that it is smaller [12, 14, 16]; or that it can be absent [24]. The G peak is also thought to represent a Fano resonance due to phonon coupling with plasmons [10, 12, 13, 24, 25]. Such phonon-plasmon coupling would either need [13] or not need [10, 25] a finite phonon wavevector for its activation. The theory of Refs. [10, 25] predicts the phonon-plasmon peak to be intrinsic in single SWNT, in contrast with [24]. On the other hand, the theory in

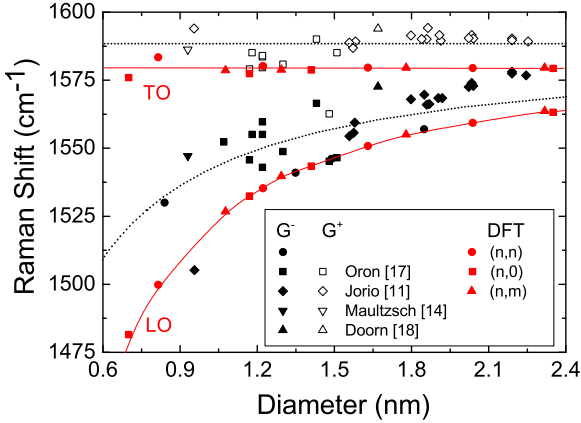


FIG. 3: (color online) Black points: experimental  $G^-$  and  $G^+$  in metallic SWNTs vs. diameter. Red points: DFT for arm chair [from (3,3) to (18,18)], zigzag [from (9,0) to (30,0)] and chiral tubes [(5,2), (12,3), (16,1), (16,10), (20,14)]. Lines: fit of Eq. 5 to the experimental and DFT data.

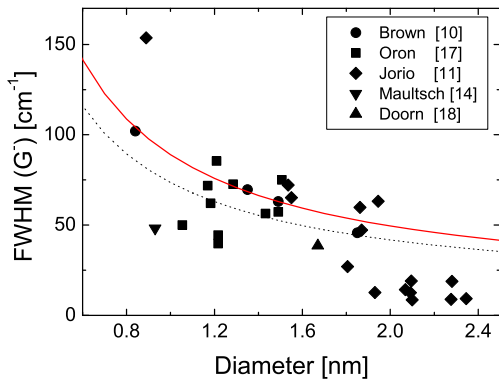


FIG. 4: Experimental FWHM ( $G^-$ ) in metallic SWNTs vs. diameter. Solid line: DFT. Dotted line: fit of FWHM =  $\frac{E_P}{\lambda_D} + \frac{a}{d}$ , with  $E_P$  from Eq. 6 and  $a = 10 \text{ cm}^{-1}$ .

Ref. [13] requires several tubes ( $> 20$ ) in a bundle in order to observe a significant  $G^-$  intensity, in contrast with the experimental observation that bundles with very few metallic tubes show a significant  $G^-$  [14, 16, 17, 18, 24]. Ref. [13] also predicts a  $G^-$  upshift with number of tubes in the bundle, in contrast with Ref. [24], which shows a downshift, and with Refs. [10, 11, 17], which show that the  $G^-$  position depends on the tube diameter and not bundle size. Finally, the  $G^-$  position predicted by [13, 25] is at least  $200 \text{ cm}^{-1}$  lower than that measured [7, 8, 9, 10, 11, 12, 14, 15, 16, 17, 18]. Thus, all the proposed theories for phonon-plasmon coupling [10, 13, 25] are very qualitative, require the guess of several physical quantities, and fail to predict in a precise, quantitative, parameter-free way the observed line-shapes and their dependence on the SWNT diameter.

We now show that, like in graphite, the EPC percentage gives the main contribution to the  $G^-$  position and FWHM, even in the absence of phonon-plasmon coupling.

Surprisingly, this has not been considered so far. However, it is clear that, if phonons do not couple to electrons, they certainly cannot couple to plasmons.

We compute the phonon frequencies for several metallic SWNTs using DFT (details are in Refs. [3, 33]). For all metallic tubes, of any chirality, we get a splitting of the modes corresponding to the graphite  $E_{2g}$  into quasi transverse (TO) and a quasi longitudinal (LO), corresponding to an atom motion tangential to the SWNT axis or parallel to it. The LO frequency is smaller than the TO and has a strong diameter dependence (Fig. 3). This is the opposite of what originally proposed, i.e. that a tangential mode should have a much stronger diameter dependence than an axial one [7, 8, 10, 11, 12, 15]. This counter-intuitive result can be understood only considering the presence of a Kohn anomaly in the phonon dispersion of metallic SWNTs [6, 33, 34]. The Kohn anomaly lowers the frequency of phonons having a significant EPC. While the LO EPC is large, the TO EPC is zero. Thus, the LO frequency is smaller than the TO. Furthermore, from the dependence of the EPC on the tube diameter [3], we get the analytic result [33]:

$$\lambda_{\text{LO}}^2 = \lambda_{\text{TO}}^2 \cdot C_M \cdot d \quad (5)$$

with  $C_M$  a constant. We thus assign the  $G^-$  peak to the LO (axial) mode and the  $G^+$  to the TO (tangential) mode. Fig. 3 compares our DFT calculations with experiments (Fig. 3). The agreement is excellent, considering that no fitting parameters are used. If we fit Eq. 5 to Fig. 3, we get  $C_M = 1.52 \times 10^5 \text{ cm}^{-2} \text{ nm}$ ;  $\lambda_{\text{TO}} = 1591 \text{ cm}^{-1}$ . Note that a  $1/d^4$  dependence of  $\lambda_G^2$  was previously suggested based on phonon-plasmon coupling [10, 11].

Now we use Eq. 1 to derive the EPC contribution to FWHM ( $G^+$ ) and FWHM ( $G^-$ ) in metallic SWNTs. The EPC of a SWNT can be obtained from the graphite EPC  $\hbar D^2 i_F$  via zone-folding (valid for  $d < 0.8 \text{ nm}$ , i.e. for the vast majority of SWNTs used in experiments and devices) [3]. Four scattering processes are involved (Fig. 2-b) and the LO and TO linewidths are:

$$\frac{E_P}{\lambda_D} = \frac{2 \cdot \frac{p}{3} \cdot a_0^2 \cdot \hbar D^2 i_F}{M \cdot d}; \quad \frac{E_P}{\lambda_{\text{TO}}} = 0: \quad (6)$$

Eq. 6 is a key result. It shows that the EPC contributes to the linewidth only for the LO mode in metallic SWNTs. For semiconducting SWNTs the EPC contribution is zero for both the TO and LO modes, since the gap does not allow to satisfy the energy conservation in Eq. 1.

This confirms our assignment of the  $G^-$  and  $G^+$  Raman peaks to the LO and TO modes. Experimentally, in semiconducting SWNTs FWHM ( $G^+$ ) and FWHM ( $G^-$ ) are similar (both are  $\sim 10 \text{ cm}^{-1}$ ), while in metallic tubes FWHM ( $G^-$ )  $\sim 60 \text{ cm}^{-1}$  and FWHM ( $G^+$ )  $\sim 10 \text{ cm}^{-1}$ , for a given  $d$  [11, 17]. The large FWHM ( $G^-$ ) in metallic SWNTs is due to the large EPC and the small FWHM ( $G^+$ ) is entirely anharmonic in origin [35]. Thus, even if

FW HM (G) in graphite and FW HM (G<sup>+</sup>) in SW NTs are similar, their origin is totally different. This also explains why a FW HM (G<sup>+</sup>) < FW HM (G) can be seen [11].

Eq. 6 explains the 1/d dependence of FW HM (G) in metallic SW NTs [11]. Then, using Eq. 6,  $hD^2 i_F$  can be directly fit from the experimental FW HM (G) (Fig. 4). We find  $hD^2 i_F = 37 \text{ (eV/A)}^2$ , again in agreement with DFT. Note that, while the DFT  $hD^2 i_F$  is that of planar graphene, the fitted  $hD^2 i_F$  is obtained from measurements of SW NTs. Thus, the good agreement between the two values is a direct verification that the SW NT EPC can be obtained by folding the graphene EPC [3].

The most common process involved in Raman scattering is single resonance. Double resonance is necessary to explain the activation of otherwise inactive phonons away from  $\omega_0$ , such as the D peak [4, 37]. It has been suggested that even the G<sup>+</sup> and G peaks in SW NTs are always double resonant [15, 36]. However, if the laser excitation energy satisfies single resonance conditions, the intensity of single resonance peaks is expected to be dominant in the Raman spectrum [38]. Double resonance can only be relevant for higher excitation energies. The condition set by Eq. 4 must also hold for SW NTs in order to have a significant EPC contribution to the linewidth. Eq. 4 can only be satisfied by phonons with wavevector too small to be double resonant [14, 15]. Thus, in double resonance, the G peak should be much narrower than experimentally observed. Interestingly, it has been reported that the broad G peak disappears by increasing the excitation energy while measuring the Raman spectrum of a metallic SW NT, and a sharper one appears [14]. We explain this as a transition from single to double resonance.

Finally, in Ref. [3] we computed the zero-temperature lifetime of a conduction electron in a SW NT, due to phonon scattering. If phonons are thermalized, determines the electron mean free path  $l_e = \tau_e v_F$  at zero temperature. The phonon linewidths can be expressed as a function of  $\omega$  as:

$$\frac{E_P}{\omega_0} = 4 = \frac{bs}{\omega_0} = 4 = \frac{fs}{\omega_0}; \quad (7)$$

where  $bs$  ( $fs$ ) indicate back (forward)-scattering [3]. Such simple relations might seem surprising. In fact, the two quantities  $\tau_e$  and  $\tau$  describe two distinct phenomena:

$\tau_e$  is the lifetime of a phonon (Eq. 1) and  $\tau$  is the lifetime of an electron (Eq. 1 of Ref. [3]). In general, one does not expect a simple relation between  $\tau_e$  and  $\tau$ . However, due to the low dimensionality, in SW NTs  $\tau_e$  determines directly  $\tau$  (Eq. 7). Thus, the measured  $\tau_e$  are also a direct measurement of  $l_e$  for metallic SW NTs. Since the measured  $\tau_e$  is in agreement with DFT calculations, the results of Ref. [3] are further confirmed.

In conclusion, we presented a set of simple formulas (Eqs. 2, 3, 6), with the graphite EPC as the only parameter. Remarkably, these formulas quantitatively explain a string of experiments, ranging from phonon slopes and FW HM (G) in graphite to G peak position

and FW HM (G) diameter dependence in SW NTs. Fitting a wide set of independent data we obtain the same EPCs  $\sim 10\%$ . These experimental EPC are in excellent agreement with, and validate, the DFT approach.

Calculations performed at HPCF (Cambridge) and IDRIS (grant 051202) are acknowledged. M. Oron and R. Kupke for useful discussions. Funding from EU IHP-HPM T-CT-2000-00209 and CANAPE, from EPSRC GR/S97613 and The Royal Society is acknowledged.

Electronic address: lazzeri@impm.cjussieu.fr

Electronic address: acf26@eng.cam.ac.uk

- [1] Z. Yao, C. L. Kane and C. D. Eckler, Phys. Rev. Lett. 84, 2941 (2000).
- [2] J. Y. Park et al., Nano Lett. 4, 517 (2004).
- [3] M. Lazzeri et al., cond-mat/0503278.
- [4] V. Perebeinos, J. Terso, P. A. Vouris, Phys. Rev. Lett. 94, 086802 (2005).
- [5] A. Javey et al., Phys. Rev. Lett. 92, 106804 (2004).
- [6] S. Piscanec et al., Phys. Rev. Lett. 93, 185503 (2004).
- [7] M. A. Pimenta et al., Phys. Rev. B 58, 16016 (1998).
- [8] H. Kataura et al., Synth. Met. 103, 2555 (1999).
- [9] P. M. R. Afanlov, H. Jantoljak, and C. Thomsen, Phys. Rev. B 61, 16179 (1999).
- [10] S. D. M. Brown et al., Phys. Rev. B 63, 155414 (2001).
- [11] A. Jorio et al., Phys. Rev. B 65, 155412 (2002); 66, 115411 (2002); M. S. Dresselhaus et al., Physica B 323, 15 (2002).
- [12] C. Jiang et al., Phys. Rev. B 66, 161404 (2002).
- [13] K. Kempa, Phys. Rev. B 66, 195406 (2002).
- [14] J. Maultzsch et al., Phys. Rev. Lett. 91, 087402 (2003).
- [15] Jorio et al.; Thomsen et al.; Reich et al.; P. Tan et al. in Raman spectroscopy in carbons: from nanotubes to diamond, eds. A. C. Ferrari and J. Robertson Phil. Trans. Roy. Soc. A 362, 2267-2565 (2004).
- [16] H. Telg et al., Proceedings of IWPENM 2005 AIP, Melville, NY, 2005.
- [17] M. Oron, R. Kupke et al., Nano Lett. in press (2005).
- [18] S. K. D. Dorn et al., Phys. Rev. Lett. 94, 016802 (2005).
- [19] T. Hertel and G. M. Oos, Phys. Rev. Lett. 84, 5002 (2000).
- [20] J. Jiang et al., Chem. Phys. Lett. 392, 383 (2004).
- [21] G. D. Mahan, Phys. Rev. B 68, 125409 (2003).
- [22] G. Pennington and N. Goldman, Phys. Rev. B 68, 045426 (2004).
- [23] J. Jiang et al., Phys. Rev. B 71, 045417 (2005).
- [24] M. Paillet et al., Phys. Rev. Lett. 94, 327401 (2005).
- [25] S. M. Bose, S. G. Ayan, S. N. Behera, cond-mat/0506004.
- [26] P. B. Allen, Phys. Rev. B 6, 2577 (1972); P. B. Allen and R. Silberglitt, ibid. 9, 4733 (1974).
- [27] J. Maultzsch et al., Phys. Rev. Lett. 92, 075501 (2004).
- [28] F. Tuinstra, J. Koenig, J. Chem. Phys. 53, 1126 (1970).
- [29] The EPC dependence on  $k$  is given in Eq. 6 of Ref. [6]. A factor 2 in Eq. 3 accounts for both  $K$  and  $K^0$ .
- [30] V. Scardaci, A. C. Ferrari, unpublished.
- [31] A. C. Ferrari and J. Robertson, Phys. Rev. B 61, 14095 (2000); ibid. 64, 075414 (2001).
- [32] P. Tan et al., Phys. Rev. B 64, 214301 (2000).
- [33] S. Piscanec et al., unpublished.
- [34] O. Dubay and G. Kresse, Phys. Rev. B 67, 035401 (2003).

- [35] FW HM (G<sup>-</sup>) and FW HM (G<sup>+</sup>) increase 15 cm<sup>-1</sup> with temperature in the 80K -600K range for both metallic and semiconducting SWNTs [11, 30]. Thus <sup>an</sup> <sub>EP</sub>.
- [36] J. Maultzsch, S. Reich, C. Thomsen, Phys. Rev. B 65 233402 (2002)
- [37] C. Thomsen, S. Reich Phys. Rev. Lett. 85, 5214 (2000).
- [38] M. A. Pimenta et al, in Proceedings of IWEPM 2003 (AIP, Melville NY, 2003).